Homework #1

Caroline Hughes

February 12, 2018

Consider the heat equation $u_t = u_{xx}$ with initial conditions $u(x,0) = \sin(\pi x)$ on [0,1] and boundary condition $u(0,t) = u(1,t) = 0$:

$$\begin{cases} u_t = u_{xx} & t \geq 0,\ 0 \leq x \leq 1 \\ u(0,t) = u(1,t) = 0 & 0 \leq x \leq 1 \\ u(x,0) = \sin(\pi x) & t \geq 0 \end{cases} \tag{1}$$

The solution can be approximated numerically by discretizing $u(x,t)$:

$$u_j^n = u(hj, nk), \qquad j = 0, 1, \ldots, J, \quad n = 0, 1, \ldots, N$$

A numerical scheme can be developed to solve Equation 1 by using central differences to approximate u_{xx}, as shown on the left and right-hand-sides of Equation 2a. After solving explicitly for u_j^n, Equation 2b can be used to find $u(x,t)$ at the next time step $n+1$ based on the solution at the current time step n.

$$u_t = u_{xx}$$

$$\frac{u_j^{n+1} - u_j^n}{k} = \frac{u_{j-1}^n - 2u_j^n + u_{j+1}^n}{h^2} \tag{2a}$$

$$u_j^{n+1} = \lambda u_{j-1}^n + (1-2\lambda)u_j^n + \lambda u_{j+1}^n, \quad \lambda \equiv \frac{k}{h^2} \tag{2b}$$

Applying the initial condition to the discretized function u_j^n, $u_0^n = u_J^n$, Equation 2b for

$$u_j^1 = (1-2\lambda)u_1^n + \lambda u_2^n$$
$$u_{J-1}^{n+1} = \lambda u_{J-2}^n + (1-2\lambda)u_{J-1}^n$$

Equation 2b can be represented for all $j \in [1, J-1]$

$$\boldsymbol{u}^{n+1} = A\boldsymbol{u}^n \tag{3a}$$

$$A = \begin{pmatrix} 1-2\lambda & \lambda & & & \\ \ddots & \ddots & & & \\ \lambda & 1-2\lambda & \lambda & & \\ & \ddots & \ddots & & \\ & & \lambda & 1-2\lambda \end{pmatrix} \tag{3b}$$

Visually, this is represented in Fig. 1.

Figure 1: Visual representation of the A matrix applied to the function of $\boldsymbol{u}(x, t = nk)$ to iterate to find the solution at the following time step

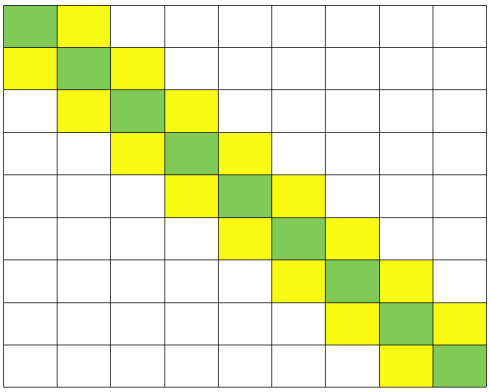

1 Stability Analysis

In general, the solution to the heat equation can be expressed in terms of the Fourier modes in time and space:

$$v(x,t) = e^{\imath\beta x}e^{\xi t} \longrightarrow v(jh, nk) = e^{\imath j\beta h}e^{n\xi k}, \quad \left|e^{\xi k}\right| \leq 1$$

where β and ξ are real constants. The numerical scheme given in Equation 2b can be expressed in terms of these Fourier modes:

$$\begin{aligned} e^{\imath j\beta h}e^{(n+1)\xi k} &= \lambda e^{\imath(j-1)\beta h}e^{(n+1)\xi k} + (1-2\lambda)e^{\imath j\beta h}e^{(n+1)\xi k} + \lambda e^{\imath(j+1)\beta h}e^{(n+1)\xi k} \\ e^{\xi k} &= \lambda e^{-\imath\beta h} + (1-2\lambda) + \lambda e^{\imath\beta h} \\ &= 1 - 2\lambda\left(1 - \cos(\beta h)\right) \\ &= 1 - 4\lambda\sin^2\left(\frac{\beta h}{2}\right) \geq 1 - 4\lambda \end{aligned}$$

The requirement that the solution must be bounded such that $\left|e^{\xi k}\right| \leq 1$ can be applied to impose stability requirements on λ:

$$e^{\xi k} \geq 1 - 4\lambda \geq -1 \quad \Longrightarrow \quad \boxed{\lambda \leq \frac{1}{2}} \tag{4}$$

1.1 $\lambda > 1/2$

In the case that $h = k = 1/10$, $\lambda = 10$ and the method is unstable. Fig. 2 shows the norm of the solution as a function of time. If the solution were stable, I would expect the norm to be bounded and the solution to decrease; however, this is not the case.

Figure 2: $\|u(x)\|_2$ vs. t

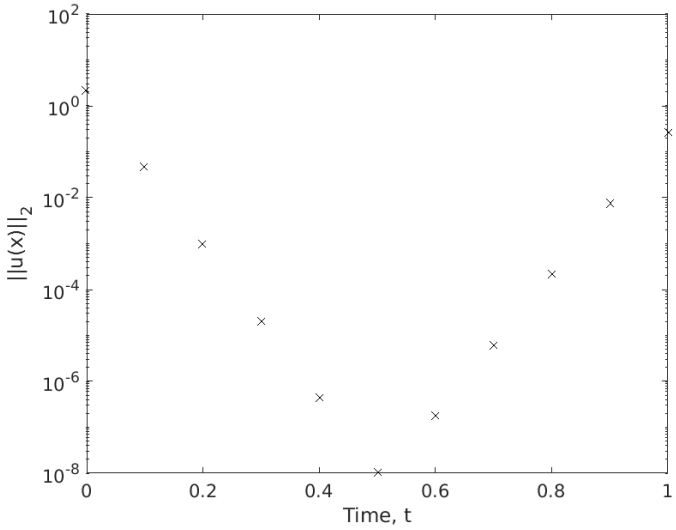

From Fig. 2, I can see that the solution is no longer stable after time $t = 0.5$. This can be seen from comparing the exact solution, derived in Section 2 and given by Equation 7, to the computed solutions at varying time steps in Figs. 3(a) to 3(d). Fig. 3(a) compares the solutions at $t = 0$ as a sanity check: the initial condition should fall exactly on the solution, as this is how the scheme begins. Fig. 3(b) compares the solutions at the following time step, $t = 0.1$, where the numeric solution is already significantly lower than the exact solution. Figs. 3(c) and 3(d) compare the solutions after $t = 0.5$, where the instability becomes apparent in Fig. 2. This instability only worsens as it is compounded with each successive time step.

(a) $t = 0$

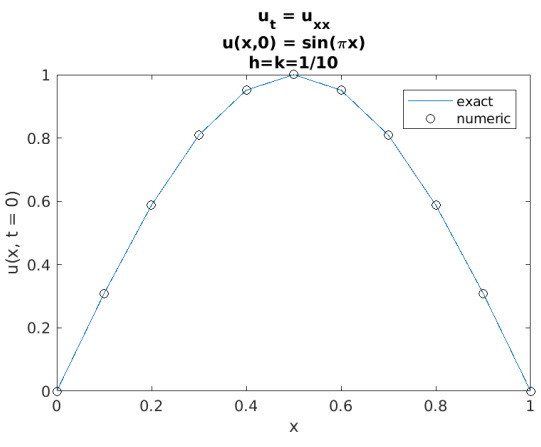

(b) $t = 0.1$

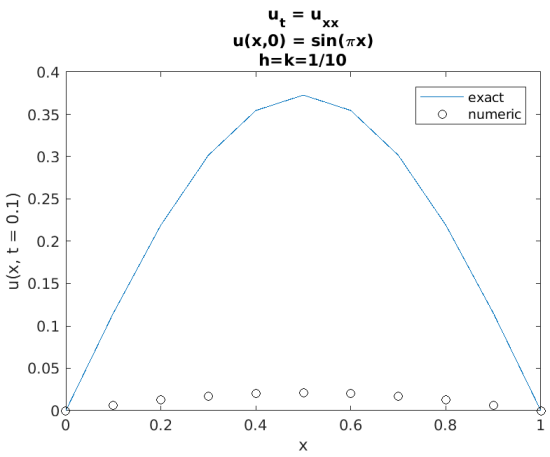

(c) $t = 0.8$

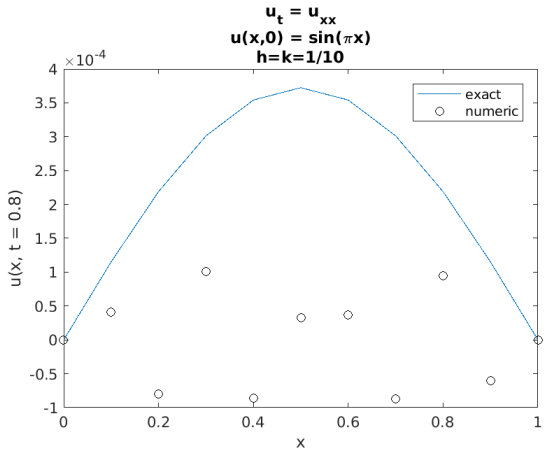

(d) $t = 1.0$

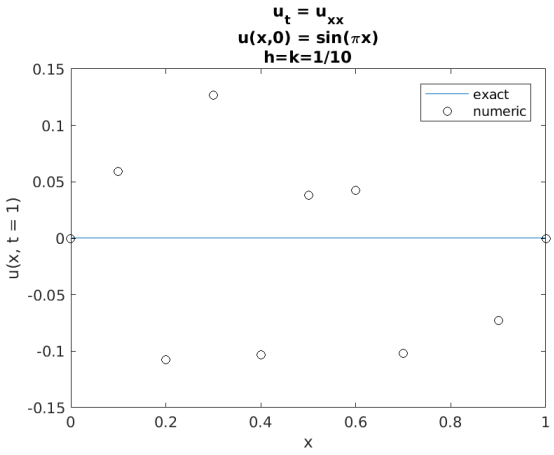

1.2 $\lambda = 1/2$

Now, after choosing a step size of $h = 1/10$ in space and $k = 1/200$ in time, $\lambda = 1/2$, falling on the border of the stability condition derived in Equation 4. Fig. 4 shows the norm of the solution as a function of time. As expected, the solution is stable and the norm decreases as a function of time.

Figure 4: $\|u(x)\|_2$ vs. t

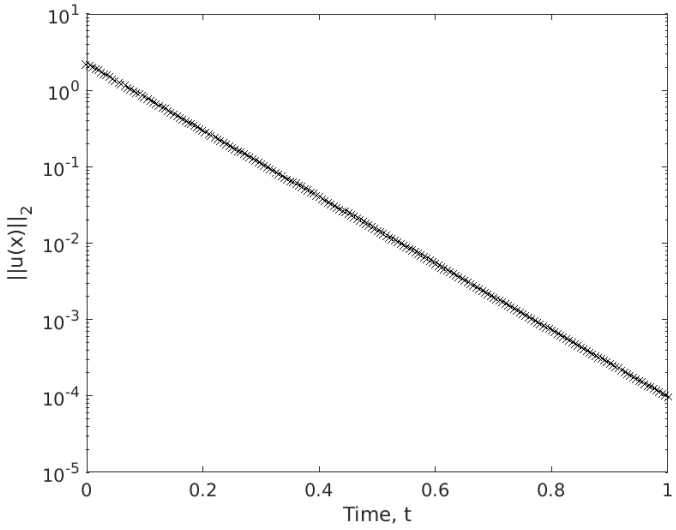

1.3 $\lambda = 1/6$

The following Taylor expansions approximate the solution $v^n_{j\pm1}$, $\pm h$ in space, or $v^{n\pm1}_j$, $\pm k$ in time, from the solution v^n_j with $\mathcal{O}(h^6)$ and $\mathcal{O}(k^6)$ accuracy.

$$u^n_{j\pm1} = u \pm hu_x + \frac{h^2}{2}u_{xx} \pm \frac{h^3}{6}u_{xxx} + \frac{h^4}{24}u_{xxxx} \pm \frac{h^5}{120}u_{xxxxx} + \mathcal{O}(h^6)$$
$$u^{n\pm1}_j = u \pm ku_t + \frac{k^2}{2}u_{tt} \pm \frac{k^3}{6}u_{ttt} + \frac{k^4}{24}u_{tttt} \pm \frac{k^5}{120}u_{ttttt} + \mathcal{O}(k^6)$$

Substituting these expressions into Equation 2b,

$$\begin{aligned}
\tau_n = \frac{1}{k}\Bigg[&\left(\cancel{u} + ku_t + \frac{k^2}{2}u_{tt} + \frac{k^3}{6}u_{ttt} + \frac{k^4}{24}u_{tttt} + \frac{k^5}{120}u_{ttttt} + \mathcal{O}(k^6)\right) - \cancel{u}\Bigg] \\
- \frac{1}{h^2}\Bigg[&\left(\cancel{u} - \cancel{hu_x} + \frac{h^2}{2}u_{xx} - \cancel{\frac{h^3}{6}u_{xxx}} + \frac{h^4}{24}u_{xxxx} - \cancel{\frac{h^5}{120}u_{xxxxx}} + \mathcal{O}(h^6)\right) - \cancel{2u} \\
&+ \left(\cancel{u} + \cancel{hu_x} + \frac{h^2}{2}u_{xx} + \cancel{\frac{h^3}{6}u_{xxx}} + \frac{h^4}{24}u_{xxxx} + \cancel{\frac{h^5}{120}u_{xxxxx}} + \mathcal{O}(h^6)\right)\Bigg] \\
= &\underbrace{u_t - u_{xx}}_{0} + \underbrace{\frac{k}{2}u_{tt} - \frac{h^2}{12}u_{xxxx}}_{0 \text{ if } \lambda=1/6} + \mathcal{O}(k^2) + \mathcal{O}(h^4)
\end{aligned}$$

$$\tau_n = \begin{cases} \mathcal{O}(k) + \mathcal{O}(h^2), & \lambda \le 1/2, \lambda \ne 1/6 \\ \mathcal{O}(k^2) + \mathcal{O}(h^4), & \lambda = 1/6 \end{cases}$$

In general, $\lambda \le 1/2$ satisfies the stability condition as shown in Equation 4 and the method is convergent of order $\mathcal{O}(k)$ in time and order $\mathcal{O}(h^2)$ in space. In the specific case of $\lambda = 1/6$, the method becomes convergent of order $\mathcal{O}(k^2)$ in time and order $\mathcal{O}(h^4)$ in space.

A numerical scheme's spatial order of convergence can be calculated when the exact solution is unknown by comparing the solutions calculated using increasingly large spatial meshes. A method is considered to be of order N, where N can be found using Equation 5.

$$\mathcal{O}\left(h^N\right): \qquad \frac{\left\|u_h - u_{h/2}\right\|_2}{\left\|u_{h/2} - u_{h/4}\right\|_2} \approx 2^N \tag{5}$$

I considered the solution evaluated at time $T = 1$ with step sizes $h = 1/10$, $h/2$, and $h/4$. I then "coarsened" the mesh for the solutions $u_{h/2}$ and $u_{h/4}$ so that they would include the solutions calculated at the same positions as in u_h. A graphical representation of this method is included in Table 1.

With each solution vector equal in length, it becomes possible to take the norms of the differences between the solutions, as is done in Equation 5. I first tried looking only at the center point of each solution vector at time $T = 1$. For this solution, error is largest at this point furthest from the boundary conditions at $x = 0$ and $x = 1$, where the solution is "anchored" to its exact value. However, I believe the method of evaluating the "coarsened" norms should be most exact for evaluating the order of convergence in general.

I examined the order of convergence for $\lambda = 1/2$, the maximum value of λ for which the method is expected to converge according to the Fourier stability condition; $\lambda = 4/9$, less than the limiting value;

Table 1: Visual representation of the solution vector for each step size, as required by Equation 5. When coarsened, only the points that align will be used to calculate the norm.

Step size	Grid points												
h	x				x				x				x
$h/2$	x		x		x		x		x		x		x
$h/4$	x	x	x	x	x	x	x	x	x	x	x	x	x

$\lambda = 1/6$, the value for which order of convergence is expected to jump to $\mathcal{O}(h^4)$; and $\lambda = 2/9$, to show that $\lambda = 1/6$ truly is a special case and that the order of convergence does not simply increase for decreasing values of λ. For each value of λ, I tested the order of convergence for $h = 1/10, 1/20, 1/40$ and $1/80$. For smaller values of λ $(= 1/6, 2/9)$, I omitted the smallest step size to spare my laptop the computational effort. The calculated orders of functions of step size are summarized in Table 2.

Table 2: Order calculated at each step size h (in reference to Equation 5) for varied λ

Step size	1/2	4/9	1/6	2/9
1/10	1.9242	1.9377	4.0101	1.9851
1/20	1.9814	1.9846	4.0025	1.9963
1/40	1.9954	1.9962	4.0009	1.9991
1/80	1.9988	1.9990		

As expected, the scheme is order $\mathcal{O}(h^4)$ for $\lambda = 1/6$, and $\mathcal{O}(h^2)$ for $\lambda < 1/2$. Fig. 5 shows the error in the calculated order of convergence as a function of the step size used in its calculation.

Figure 5: Error in order of convergence as a function of step size

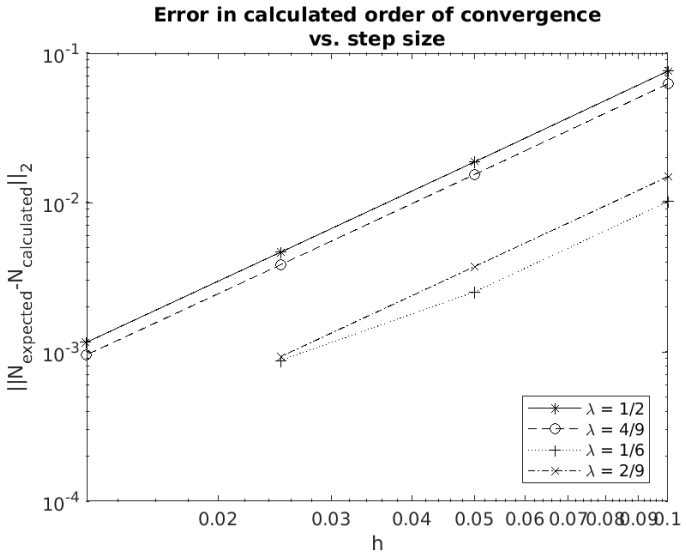

From Fig. 5, it is clear that decreasing the step size monotonically decreases the error.

2 Fourier Series Solution: Sinusoidal Initial Condition

In general, the heat equation with the initial condition $u(0,t) = u(1,t) = 0$ can be solved using separation of variables, $v(x,t) = F(x)G(t)$, to find the Fourier series solution. I'll solve the version of the heat equation including the constant α as is done in Equation 10, to find a more general solution. Here, I will use the notation $v(x,t)$ to indicate that this solution is exact.

$$\frac{1}{\alpha F(x)G(t)}\left(F(x)\frac{dG}{dt}\right) = \left(\alpha G(t)\frac{d^2F}{dx^2}\right)\frac{1}{\alpha F(x)G(t)}$$

$$\frac{1}{\alpha G(t)}\frac{dG}{dt} = \frac{1}{F(x)}\frac{d^2F}{dx^2} = -q^2$$

Time-dependent term:

$$\frac{dG}{dt} = -\alpha q^2 G(t) \quad \Longrightarrow \quad G(t) = G(0)e^{-\alpha q^2 t}$$

Spatial term:

$$\frac{d^2F}{dx^2} = -q^2 F(x) \quad \Longrightarrow \quad F(x) = a\cos(qx) + b\sin(qx)$$

Apply boundary conditions:

$$F(0) = a = 0 \quad \Longrightarrow \quad a = 0$$
$$F(1) = b\sin(q) = 0 \quad \Longrightarrow \quad \sin(q_n) = \sin(n\pi) \quad \Longrightarrow \quad q_n = n\pi$$

where n is an integer. Combining the spatial and time solutions:

$$v_n(x,t) = \underbrace{b_n G(0)}_{b_n} e^{-\alpha q_n^2 t}\sin(q_n x)$$

$$v(x,t) = \sum_{n=1}^{\infty} b_n e^{-\alpha(n\pi)^2 t}\sin(n\pi x) \tag{6}$$

Applying the initial condition to determine the Fourier coefficients,

$$v(x,0) = \sum_{n=1}^{\infty} b_n \sin(n\pi x) = \sin(\pi x)$$

This can only be true if the complete Fourier series solution is truncated at $n = 1$ with $b_1 = 1$.

$$\boxed{v(x,t) = e^{-\pi^2 t}\sin(\pi x)} \tag{7}$$

The exact solution includes only the first term of the Fourier series, so this should already evaluate the solution to a degree of accuracy better than any achievable numerically. The exact solution calculated here was used to compare the numerical and exact solutions in Figs. 3(a) to 3(d).

3 Fourier Series Solution: Quadratic Initial Condition

The analytical solution to the heat equation becomes more interesting with the initial condition:

$$\begin{cases} u_t = u_{xx}, & t \geq 0,\ 0 \leq x \leq 1 \\ u(0,t) = u(1,t) = 0, & 0 \leq x \leq 1 \\ u(x,0) = x(1-x), & t \geq 0 \end{cases} \tag{8}$$

Starting from the general Fourier series solution to $u_t = u_{xx}$ and applying this initial condition,

$$v(x,0) = \sum_{n=1}^{\infty} b_n \sin(n\pi x) = x(1-x)$$

where

$$b_n = 2\int_0^1 x(1-x)\sin(n\pi x)dx = 2\left[\int_0^1 x\sin(n\pi x)dx - \int_0^1 x^2\sin(n\pi x)dx\right]$$

$$\int_0^1 x\sin(n\pi x)dx = \frac{1}{n\pi}\Bigg[-\underbrace{x\cos(n\pi x)\Big|_0^1}_{(-1^n)} + \underbrace{\int_0^1 \cos(n\pi x)dx}_{0}\Bigg] = -\frac{(-1)^n}{n\pi}$$

$$\int_0^1 x^2\sin(n\pi x)dx = \frac{1}{n\pi}\Bigg[-\underbrace{x^2\cos(n\pi x)\Big|_0^1}_{(-1)^n} + 2\int_0^1 x\cos(n\pi x)dx\Bigg]$$

$$= \frac{1}{n\pi}\Bigg\{ -(-1)^n + \frac{2}{n\pi}\Bigg[\underbrace{x\sin(n\pi x)\Big|_0^1}_{0} - \int_0^1 \sin(n\pi x)dx\Bigg]\Bigg\}$$

$$= -\frac{(-1)^n}{n\pi} + \frac{2}{n^3\pi^3}\underbrace{\cos(n\pi x)\Big|_0^1}_{(-1)^n - 1} = -\left[\frac{(-1)^n}{n\pi} + \frac{2}{n^3\pi^3}\left(1-(-1)^n\right)\right]$$

$$b_n = 2\left\{ -\cancel{\frac{(-1)^n}{n\pi}} + \left[\cancel{\frac{(-1)^n}{n\pi}} + \frac{2}{n^3\pi^3}\left(1-(-1)^n\right)\right]\right\} = \frac{4}{n^3\pi^3}\left(1-(-1)^n\right) = \begin{cases} \left(\dfrac{2}{n\pi}\right)^3 & \text{odd } n \\ 0 & \text{even } n \end{cases}$$

By redefining $n \to 2n-1$, everywhere it appears in the Fourier series solution, I can ensure that all of the terms are non-zero and satisfy the initial condition. The final result is now:

$$\boxed{v(x,t) = \sum_{n=1}^{\infty}\left(\frac{2}{(2n-1)\pi}\right)^3 e^{-(2n-1)^2\pi^2 t}\sin\left((2n-1)\pi x\right)} \tag{9}$$

Fig. 6 shows the numeric and analytic solutions at the initial and final times. I plotted the Fourier series solution at the initial condition to show that this is in fact the correct analytic solution even though the solution at time $t = 1$ is consistently lower than the numeric solution. I found this to be true whether I chose to truncate the Fourier series at $n = 5$ or $n = 50$; however, I did strategically choose to truncate at $n = 5$.

Figure 6: Comparison of the numeric solution to Equation 8 calculated with $\lambda = 1/2$ and the analytic Fourier series solution

(a) $t = 0$ (b) $t = 1$

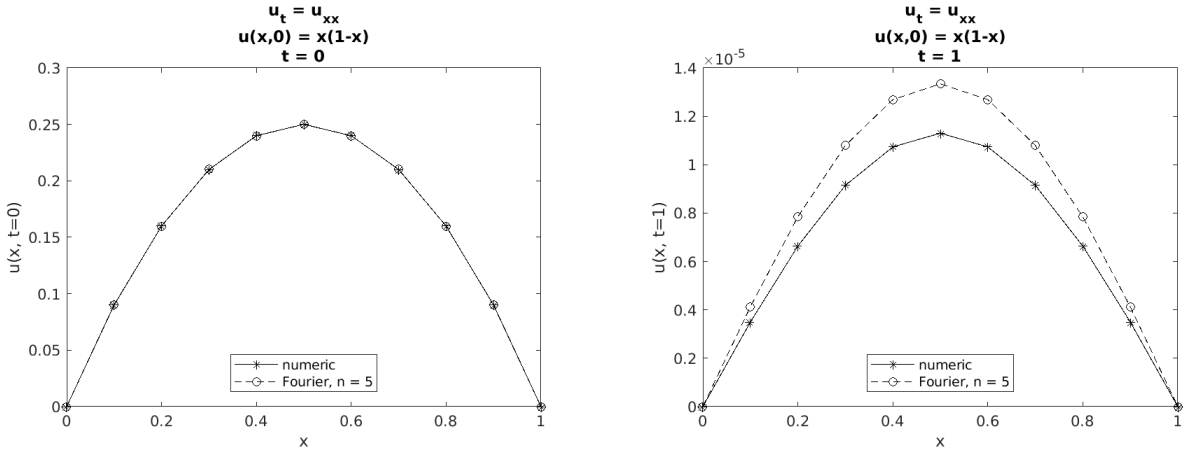

Truncation Gottlieb et al. state "the Fourier series of an analytic and periodic function, truncated after $2N + 1$ terms, converges exponentially with N"[1]. They elaborate that the further a function deviates from periodic, the more the Fourier series deviates from this convergence pattern [1]. The initial condition in Equation 8 is quadratic and, while this is not periodic, it does resemble the function $\sin(\pi x)$ in both shape and boundary conditions, so I will assume that Gottlieb et al.'s assertation applies rather well to this situation. Therefore, I postulate that an accuracy of order $\mathcal{O}(h^2)$ will require truncating the Fourier series solution at $n = 5$ and an accuracy of order $\mathcal{O}(h^4)$ will require truncating at $n = 9$.

From inspection of Fig. 6(b), it appears that no number of terms included in the Fourier series solution will help these solutions match.

4 Non-unity diffusion coefficient

Consider $u_t = \alpha u_{xx}$ with $u(x, 0) = sin(\pi x)$ on [0,1], and boundary condition $u(0, t) = u(1, t) = 0$ (Here, α is a constant).

$$\begin{cases} u_t = \alpha u_{xx}, & t \geq 0,\ 0 \leq x \leq 1 \\ u(0,t) = u(1,t) = 0, & 0 \leq x \leq 1 \\ u(x,0) = \sin(\pi x), & t \geq 0 \end{cases} \tag{10}$$

A numerical scheme can be developed to incorporate the diffusion coefficient α, following the same steps to develop Equations 2a and 2b:

$$u_t = \alpha u_{xx}$$

$$\frac{u_j^{n+1} - u_j^n}{\alpha k} = \frac{u_{j-1}^n - 2u_j^n + u_{j+1}^n}{h^2} \tag{11a}$$

$$u_j^{n+1} = s u_{j-1}^n + (1 - 2s) u_j^n + s u_{j+1}^n, \quad s \equiv \frac{\alpha k}{h^2} \tag{11b}$$

[1] Gottlieb et al. actually begins by saying this is a well known fact, but I did not know this before discovering their paper.

The same vector equation described in Equations 3a and 3b can still be used to solve the heat equation simultaneously over all space, but now with λ replaced by s as defined in Equation 11b.

Stability condition The Fourier stability analysis followed in Section 1 can be applied to the scheme described by Equation 11b, following the steps used to find Equation 4.

$$\begin{aligned} e^{ij\beta h}e^{(n+1)\xi k} &= \alpha\lambda e^{\imath(j-1)\beta h}e^{(n+1)\xi k} + (1-2\alpha\lambda)e^{\imath j\beta h}e^{(n+1)\xi k} + \alpha\lambda e^{\imath(j+1)\beta h}e^{(n+1)\xi k} \\ e^{\xi k} &= \alpha\lambda e^{-\imath\beta h} + (1-2\alpha\lambda) + \alpha\lambda e^{\imath\beta h} \\ &= 1 - 2\alpha\lambda\left(1-\cos(\beta h)\right) \\ &= 1 - 4\alpha\lambda\sin^2\left(\frac{\beta h}{2}\right) \geq 1 - 4\alpha\lambda \end{aligned}$$

The requirement that the solution must be bounded such that $\left|e^{\xi k}\right| \leq 1$ can be applied to impose stability requirements on λ:

$$e^{\xi k} \geq 1 - 4\alpha\lambda \geq -1 \quad \Longrightarrow \quad \boxed{\lambda \leq \frac{1}{2\alpha}} \tag{12}$$

5 Variable diffusion coefficient

In addition to a diffusion coefficient $\alpha \neq 1$, it is possible to have a variable diffusion coefficient $\alpha(x)$ that changes as a function of position in the material.

$$\begin{cases} u_t = \alpha(x)u_{xx} & t \geq 0,\ 0 \leq x \leq 1 \\ u(0,t) = u(1,t) = 0 & 0 \leq x \leq 1 \\ u(x,0) = \sin(\pi x) & t \geq 0 \end{cases} \tag{13}$$

This might occur in the case of two different materials, such as an oven mitt gripping a hot sheet of fresh-baked cookies. In this case, it is important to consider the diffusion coefficients of each the mitt, sheet pan, and cookies independently. Of course, the initial and boundary conditions would be different in this scenario: the initial condition on the temperature of the cookies on the pan would be a function of temperature distribution at the time the sheet slides into the oven, and boundary conditions of $x(0,t) = x(1,t) = 0$ would indicate an oven in desperate need of repair.

Smooth diffusion coefficient Imposing a step size of $k = 1/400$ in time, h can be selected such that Equation 12 is satisfied for all values of α:

$$h = \frac{1}{\sqrt{k\max\alpha(x)/\rho}}$$

where $\rho = 4/9$ is the value I've chosen to limit $\lambda\max\alpha(x)$. I tested this for two cases of $\alpha(x)$ as shown below.

It would be possible to assess the order of convergence of the method using the process followed in Section 1. This method is limited by the maximum value of the diffusion coefficient and will therefore limit

Figure 7: Smooth $\alpha(x)$

(a) $\alpha(x) = \frac{x}{2}$

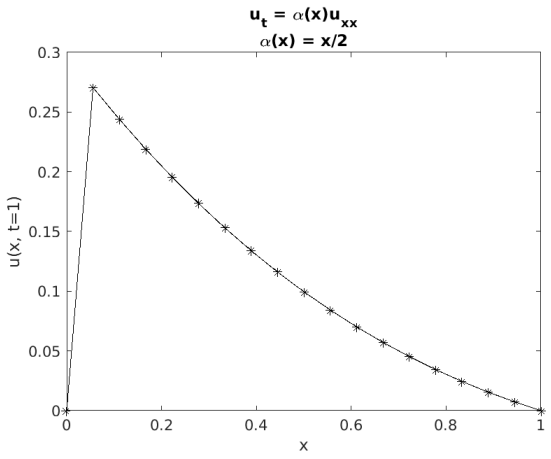

(b) $\alpha(x) = \frac{1}{2}\left|x - \frac{1}{2}\right|$

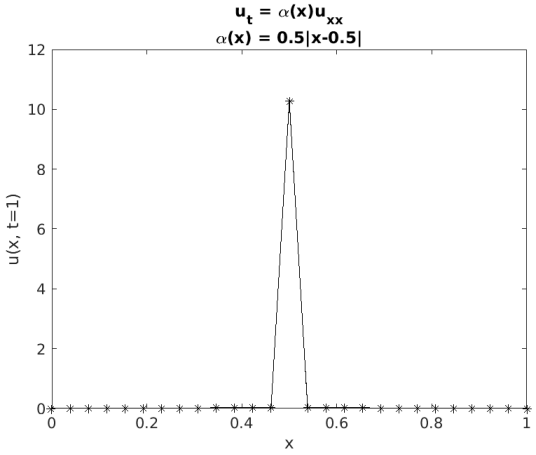

the accuracy of the method. Using an adaptive mesh size to select h based on localized values of α would be a better method that could address this limitation.

Step function without continuity At the interface, I use double forward and backward differences when approaching the interface from the left and the right, respectively. This aims to ensure more "information" comes from the side of the interface where the diffusion coefficient is better defined. In the matrix equation, this looks like:

$$\begin{pmatrix} u_{j-1}^{n+1} \\ u_j^{n+1} \\ v_j^{n+1} \\ v_{j+1}^{n+1} \end{pmatrix} = \begin{pmatrix} \alpha\lambda & 1-2\alpha\lambda & \alpha\lambda & & & \\ \alpha\lambda & 1+\alpha\lambda & \alpha\lambda & & & \\ & & & \beta\lambda & 1+\beta\lambda & \beta\lambda \\ & & & \beta\lambda & 1-2\beta\lambda & \beta\lambda \end{pmatrix} \begin{pmatrix} u_{j-1}^{n} \\ u_j^{n} \\ v_j^{n} \\ v_{j+1}^{n} \end{pmatrix}$$

Here, I am calling α and β the diffusion coefficients on the left and right of the interface and the solutions to the heat equation u_j^n and v_j^n on the left and right of the interface. I am assuming no interaction whatsoever between the information across the interface and am therefore solving twice for the point directly on the interface[2].

A few concerns arise. First, I now realize that it does not make physical sense for a continuous scheme to become discontinuous without interference from an outside forcing function. In creating this method, I assumed no crossover

At the interfaces, I use double forward and double backward differences rather than central differences to approximate the second-order spatial derivative. Each of these methods is of order $\mathcal{O}(h)$, rather than order $\mathcal{O}(h^2)$, thus dimisnishing the order of convergence for the entire scheme. I could address this by implementing a multigrid method just at the interface and patching together the points on either side.

[2]I now realize this would make more sense for a discontinuous *initial* condition rather than a diffusion coefficient.

Figure 8: A matrix visualization

(a) Two diffusion coefficients

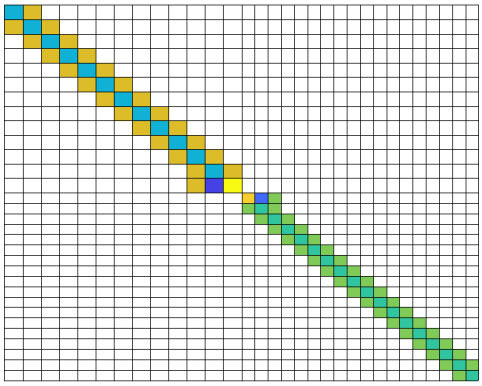

(b) Three diffusion coefficients

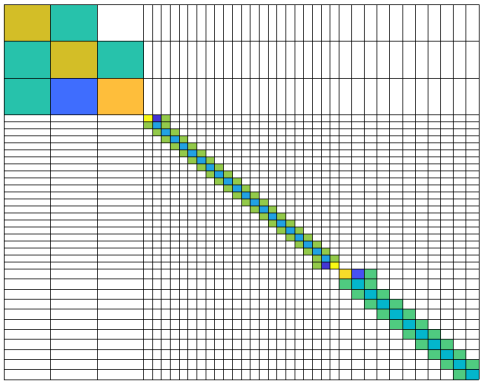

Figure 9: $u(x, t = 1)$

(a) Two diffusion coefficients

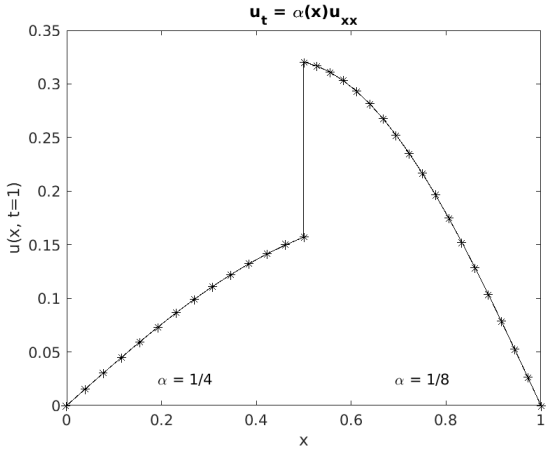

(b) Three diffusion coefficients

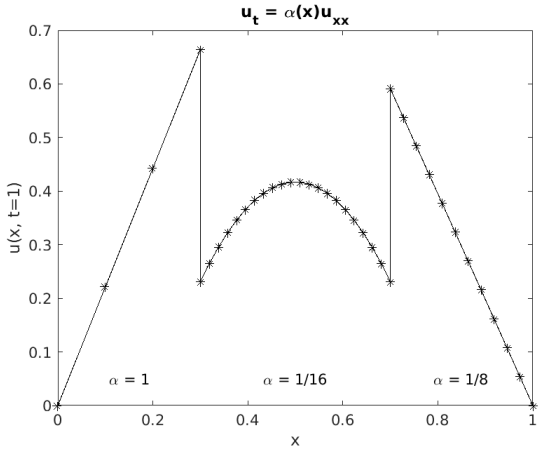

References

[1] David Gottlieb et al. "On the Gibbs phenomenon I: recovering exponential accuracy from the Fourier partial sum of a nonperiodic analytic function". *Journal of Computational and Applied Mathematics* 43.1 (1992), pp. 81 –98. ISSN: 0377-0427. DOI: 10.1016/0377-0427(92)90260-5. URL: http://www.sciencedirect.com/science/article/pii/0377042792902605.